PROCEEDINGS, 48th Workshop on Geothermal Reservoir Engineering
Stanford University, Stanford, California, February 6-8, 2023
SGP-TR-224

Thermodynamic and Transport Properties of Geothermal Fluids from South Russia Geothermal Field

Abdulagatov Ilmutdin[1,2]*, Aliev Rasul[3,4], Badavov Gasan[1]

[1]Institute for Geothermal Research and Renewable Energy of Joint Institute for High Temperatures of the Russian Academy of Sciences, 367030, Makhachkala, Russia

[2]Department of Physical and Organic Chemistry, Dagestan State University, Makhachkala, Russian Federation;

[3]Dagestan State Technical University, Makhachkala, Russian Federation

[4]OOO Geoekoprom Ltd, 367030, Makhachkala, Russia

[*1]Institute for Geothermal Research and Renewable Energy of Joint Institute for High Temperatures of the Russian Academy of Sciences, 367030, Makhachkala, Russia.

ilmutdina@gmail.com

Keywords: Geothermal fluids; Density; Thermodynamic properties; Vibrating tube densimeter; Speed of sound; Viscosity.

ABSTRACT

Volumetric (density), acoustic (speed of sound), and transport (viscosity) properties of natural geothermal fluids from south Russia Geothermal Field (Dagestan, Caspian seashore) have been measured over the temperature range from (278 to 343) K and at atmospheric pressure. The measurements were made using the Anton Paar DMA4500 densimeter and Stabinger SVM3000 viscometer for 4 geothermal fluid samples from the hot-wells Izberbash (No.68 and 129) and Ternair (No.27T and 38T). A sound-speed analyzer (Anton Paar DSA 5000) was used to measure the speed of sound and the density of the same geothermal samples. The combined expanded uncertainty of the density, viscosity, and speed of sound measurements at the 95 % confidence level with a coverage factor of $k = 2$ is estimated to be- density: 0.0005 % (for DMA 4500 densimeter), 0.02 % or 0.5 kg·m^{-3} (for the SVM 3000 viscodensimeter) and 0.01 % (for the DSA 5000 M sound-speed analyzer); viscosity - 0.35 % (for SVM 3000); and speed of sound - 0.1 % (DSA 5000 M), respectively. Measured values of density and speed of sound were used to calculate other very important for geothermal modeling derived thermodynamic properties such as adiabatic coefficient of bulk compressibility, coefficient of thermal expansion, thermal pressure coefficient, isothermal coefficient of bulk compressibility, isochoric heat capacity, isobaric heat capacity, enthalpy difference, partial pressure derivative of enthalpy, partial derivatives of internal energy (internal pressure) of the geothermal fluid samples. Measured values of density, viscosity, and speed of sound were used to develop correlation models which reproduced the measured values within 0.03 % (density), 2.55 % (viscosity), and 0.06 % (speed of sound), respectively. The measured properties at atmospheric pressure have been used as a reference values for prediction high-pressure properties.

Topics: Geosciences, application of geophysics, geochemistry, thermodynamics and fluid mechanics.

1. INTRODUCTION

The thermodynamic and transport properties of geothermal fluids are very important for determining the natural state of a geothermal system and its behavior under exploitation. Geothermal power plants use geothermal fluids as a resource and create waste residuals as part of the power generation process. Both the geofluid resource and waste stream are considered produced fluids. The chemical and physical nature of produced fluids can have a major impact on the geothermal power industry and influence the feasibility of power development, exploration approaches, plant design, operating practices, and reuse/disposal of residuals. Geothermal heat and power plants use hot geothermal fluids as a transport medium to extract thermal energy from the deep underground. A downhole pump in the production well lifts the brine up to the surface, where it is cooled in heat exchanger and reinjected subsequently (binary geothermal cycles). Knowledge of the thermophysical properties of geothermal brines is extremely important for determination of design characteristics and sizes of the downhole pump (Saadat et al., 2008). The flow characteristics (multiphase underground flows) of the brine in the well depends on their thermal properties, such as density and viscosity. The thermodynamic and transport property data of geothermal brines are also needed for geothermal energy utilization devices. Geothermal energy production operations require the ability to predict the thermodynamic properties of the geothermal brines as a function of temperature, pressure, and concentration. Particularly, knowledge of the geothermal fluid properties is important in geothermal exploration and energy production, to establish optimal operations for the productions of geothermal brine fields. For example, the total heat content of geothermal fluid depends on the density, temperature, and heat capacity (Schröder et al., 2015). For the effective utilization of geothermal resources, a precise thermodynamic and transport properties data are required for the initial resource estimates, production and reservoir engineering study of the geothermal field, reservoir modeling, and power cycle optimization.

Thermodynamic and transport properties (density, heat capacity, viscosity, thermal conductivity, *etc.*) of geothermal fluids determine the transfer of heat and mass by geothermal systems. The energy properties of the geothermal fluids may be extracted directly from the *PVTx* properties of the geothermal fluid through standard thermodynamic approaches (Haas, 1976a, b). The available *PVTx* properties

of geothermal fluids are not sufficient to meet the needs of the geothermal industry for complex solutions such as those found in geothermal reservoirs. Modeling geothermal wells (geothermal engineering, geothermal or reservoir installations) need accurate thermophysical property data (Reindl et al., 2009; Stefánsson et al., 2012). Thus, one of the key factors when planning the exploitation of geothermal resources is the availability of reliable thermodynamic and transport properties data of geothermal brines. Initially geothermal fluids were modeled as pure water. Thermodynamic and transport properties of pure water are well-known (see IAPWS formulations for thermodynamic and transport properties, Wagner and Pruß, 2002; Huber et al., 2009; and Huber et al., 2012). Used pure water or geothermal brine models (synthetic brines like binary or ternary aqueous salt solutions) properties leads to inaccuracies and impossible accurately estimate the effect all of the dissolved salts on the thermophysical properties due to extremely complexities. Also, the presence of the dissolved gases in geothermal fluids considerable influencing the thermodynamic properties. Due to pressure difference between underground and the near surface conditions (geothermal operations at 0.101 MPa), degassing occurs during geothermal energy production. Thermophysical properties of geothermal fluids such as density, viscosity, heat capacity, and enthalpy play a fundamental role in mass and heat transfer in the Earth'sinterior. In order to provide numerical modelling of the heat and mass flow processes in various geothermal energy generating (production) systems (reservoirs, pipe systems, power plants, binary geothermal cycles, heat-exchangers) definitions of the thermodynamic properties of density (ρ), viscosity (η), and enthalpy (H) of geothermal fluids as a function of temperature, pressure, and concentration are required (McKibbin and McNabb, 1995; Palliser, 1998; Palliser and McKibbin, 1998a,b; Dolejs and Manning, 2010). Solution of the set of differential equations (equations of mass conservation, linear momentum, and energy conservation), which may be used to describe the transport of mass and heat in a porous media for mathematical simulations of the Earth's interior, considerably depends on thermodynamic properties of geothermal brines (density, enthalpy, and viscosity) as a function of temperature, pressure, and concentration of salt (minerals). Solving these sets of equations enables the determination of such quantities as temperature and pressure gradients at a point in the flow, and *T, P, x* profile in time and space (Francke and Thorade, 2010; Francke et al., 2013). However, solving these equations requires knowledge of the thermodynamic properties of density, enthalpy, and viscosity of the geothermal fluids. Since the measurements in this work were performed at atmospheric pressure, the present study is not considering the effect of dissolved gases on the thermophysical properties of geothermal brines. High pressure measurements or reliable high pressure predictive models are needed for heat and mass transfer phenomena study in Earth interior.

Viscosity and density are key factors in fluid flow simulation (influencing the flow of reservoir fluids). Relatively little data has been published on the viscosity of natural geothermal brines. Most reported data only for binary or ternary aqueous salt solutions (see review Abdulagatov and Assael, 2009) as a main component of geothermal brines (basically for synthetic geothermal brines). Adams and Bachu (2002) reviewed various functions for the calculation of geothermal brine density and viscosity. Battistelli (1992), Battistelli et al. (1993), and Oldenburg et al. (1995) also described models of brines flows that require knowledge of the three key thermodynamic properties (density, viscosity, and enthalpy). Because of the scarcity of data for the density, dynamic viscosity, and enthalpy a different approach to the one used for these properties was adopted (Dittman, 1977; McKibbin and McNabb, 1995; Palliser and McKibbin, 1998a,b). Potter and Haas (1977) indicated that geothermal fluids might be represented by the properties of aqueous NaCl solution as a model of the geothermal brine. This model predicts the density of geothermal brines and seawater within experimental uncertainty at a temperature of 150 °C. The simplest way of determining of the thermodynamic properties of geothermal fluids is based on pure water properties, because pure water is the dominant constituent, therefore, governs the properties (thermodynamic behavior) of aqueous salt solutions and geothermal brines. Most reliable predictive models for aqueous salts solutions are representing their thermodynamic properties relative to pure water (Wahl, 1977; Horvath, 1985; Aseyev and Zaytsev, 1996; Aseyev, 1998; Abdulagatov et al., 2005a), because the behavior of the thermodynamic properties of geothermal brines also governs by the properties of pure water (see below Figs. 1 to 4).

Using direct experimental thermodynamic data for particular natural geothermal fluids allows minimize the errors arising from the empirical prediction data for geothermal brines models. Moreover, the brine composition can be changed during production. Thus, more direct measurements of the natural geothermal brines from various regions of the world with various concentrations of dissolved salts are needed. This allows generalize the properties of geothermal fluids from various geothermal fields (wells) with various solutes to develop prediction models for geothermal brines with any chemical composition. Unfortunately, available theoretical models frequently cannot describe real systems such as those met in practice. For example, the accurate prediction of the thermodynamic and transport properties of complex multicomponent ionic aqueous solutions such as geothermal fluids is extremely difficult due to complexity of the intermolecular interactions between water molecules and various types of salt ions. Better predictive models for practical applications can be developed based on reliable direct experimental information on thermodynamic and transport properties of natural geothermal brines. However, a literature survey reveals that very little information has been reported previously on the direct measurements of the density and viscosity of real (natural) multicomponent geothermal brines from various Geothermal Fields of the World.

The experimental study of the thermodynamic properties of each geothermal fluid would, however, be a formidable task, and theoretical or semi-empirical models that would predicted the thermodynamic properties of complex geothermal brines would be useful.

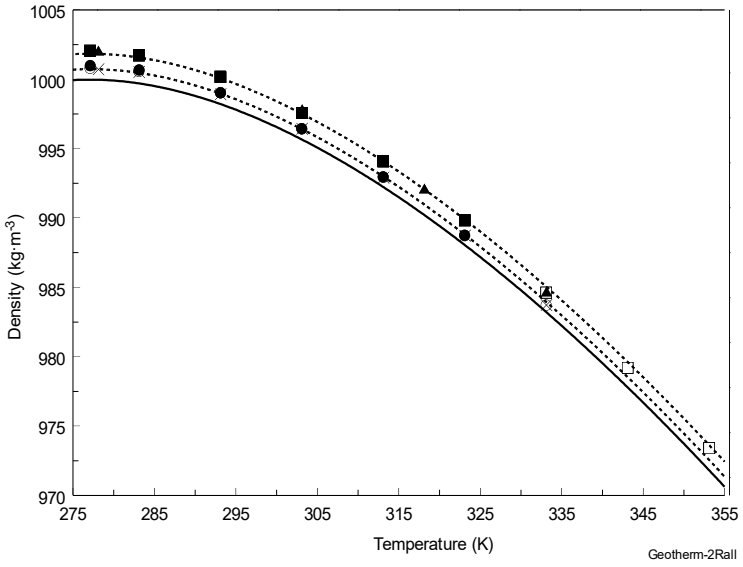

Figure 1: Measured values of density of geothermal fluids together with the values for pure water calculated from IAPWS formulation. Solid line is pure water values calculated from the IAPWS fundamental equation of state (Wagner and Pruß, 2002). Dashed lines are calculated from the correlation model Eq. (1) for the samples No.68 and No.129. × –No.68 (DSA); ○-No.68 (SVM); ●-No.68 (DMA); ■-No.129 (DMA); □-No.129 (DSA); ▲-No.129 (DSA)..

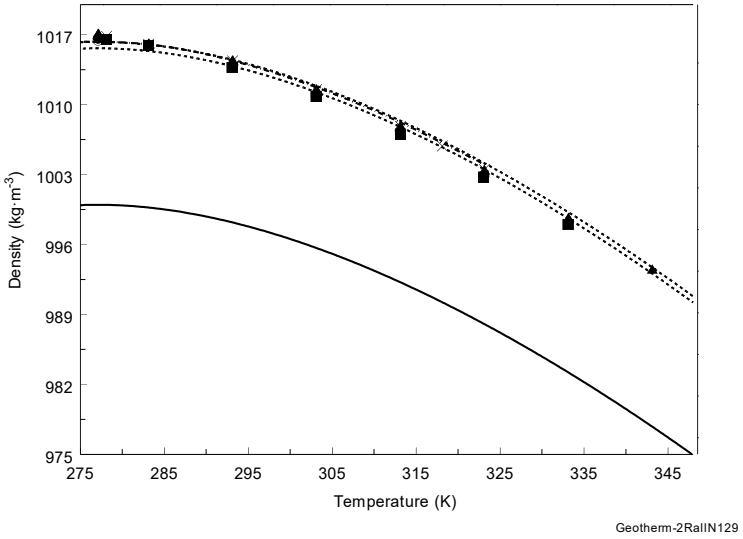

Figure 2: Measured values of density of geothermal fluids together with the values for pure water calculated from IAPWS formulation. Solid line is pure water values calculated from the IAPWS fundamental equation of state (Wagner and Pruß, 2002). Dashed lines are calculated from the correlation model Eq. (1) for the samples No.27T and No.38T. Dashed-dotted line is calculated from the model by Rogers and Pitzer (1982). ○-No.27T (SVM); ●-No.27T (DMA); ■-No.27T (DSA); × –No.38T (DSA); □-No.38T (DMA); ▲-No.38T (SVM).

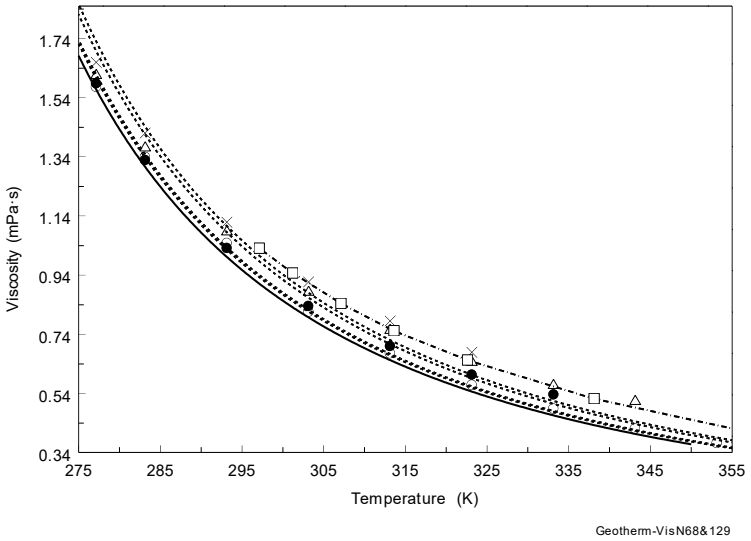

Figure 3: Measured values of viscosity for geothermal fluids together with the values for pure water calculated from IAPWS formulation. Solid line is pure water values calculated from the IAPWS correlation (Huber et al., 2009). Dashed lines are calculated from the correlation model Eq. (3). × –No.27T; △-No.38T; ○-No.129; ●-No.68; □- Kestin and Shankland (1984) for H_2O+NaCl solution.

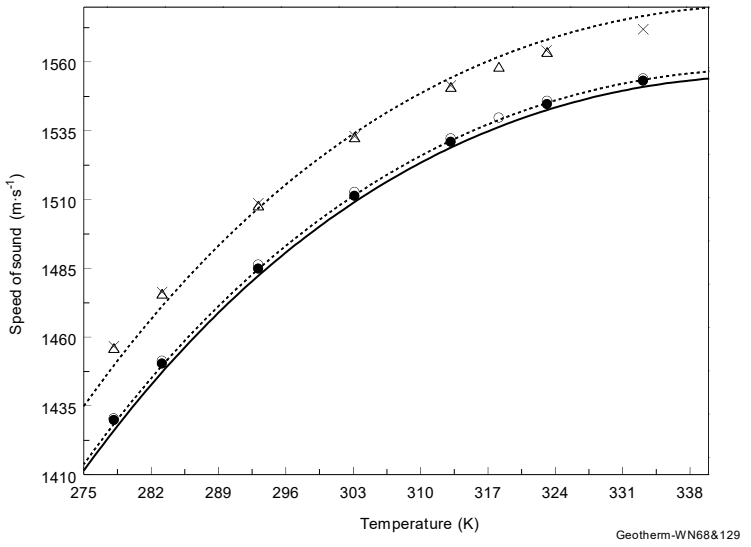

Figure 4: Measured speed of sound for various geothermal fluids together with the values for pure water calculated from IAPWS formulation. Solid line is pure water values calculated from the IAPWS correlation (Wagner and Pruß, 2002). Dashed lines are calculated from the correlation model Eq. (2). ×–No.27T; △-No.38T; ○-No.129; ●-No.68.

Francke and Thorade (2010) studied the sensitivity of the volumetric flow rate of a downhole pump in a geothermal production well on different density and viscosity functions during the startup and stationary operating phases. Used pure water or geothermal brine models (synthetic brines like binary or ternary aqueous salt solutions) properties leads to inaccuracies. The geothermal fluid was modeled as an aqueous sodium chloride solution and functions for its density and viscosity are compared and applied to a model of the geothermal fluid cycle (stationary model of a geothermal water loop). The study showed that the deviations between different density functions are up to 52% of the volumetric flow rate. Presence of dissolved ions in water at various temperatures causes the reservoir flow properties to considerably deviate from those of pure water or model solution.

Since the number of different brines encountered is large, detailed measurements on all of them become impractical. Consequently, the ability to predict the properties of brines from theories or models based on a few key aqueous electrolyte solutions is essential to the technical development of geothermal resources. Unfortunately, there is no theoretical guidance for the temperature, pressure, and oncentration dependences of the thermodynamic properties of multicomponent geothermal brines. Thus, its evaluation is based on the measured data only. Different predictive models were proposed by various authors (Piwinskii et al., 1977; Ershaghi et al., 1983;

Ostermann et al., 1986; McCain, 1991; Alkan et al., 1995; Champel, 2006; Palliser, 1998; Lee, 2000; Dolejs and Manning, 2010; Francke and Thorade, 2010; Palliser and McKibbin, 1998a,b; Spycher and Pruess, 2011; Muller and Weare, 1999; Battistelli, 2012; Milsch et al., 2010) to represent the effect of temperature, pressure, and concentration on the thermodynamic properties of geothermal fluids. All of these models based on thermodynamic properties of synthetic aqueous binary or ternary solutions, basically NaCl, since sodium chloride is the major solute in geothermal brines. Milsch et al. (2010) studied density and viscosity of synthetic geothermal brines containing varying amounts (5 mol/kg NaCl and $CaCl_2$, and 4 mol/kg KCl) of dissolved NaCl, KCl, and $CaCl_2$ salts using Höppler-viscometer and a combination of volumetric and mass measurements for density. These systematic measurements with the three aqueous salt solutions yielded calibration of mixing rules, stoichometrically weighting the individual viscosities measured at the total of the mixture for density and viscosity. The predictions when applied to a natural geothermal brine of specific chemical composition, showed good agreement with direct measurements performed with this geothermal fluid. The method allows estimate the density and dynamic viscosity of a given geothermal fluid once the chemical composition has been determined. However, this model does not taking into account the effect of dissolved gases. Further direct measurements of the thermophysical properties of the natural geothermal brines with complex compositions are needed to confirm applicability and accuracy of the mixing rules developed by Milsch et al. (2010). Ershaghi et al. (1983) reported viscosity data for synthetic brines consisting of sodium chloride, potassium chloride, and calcium chloride at concentrations from (0.99 to 16.667) wt.% and at temperatures up to 275 °C. Measurements were made using a high-temperature capillary tube designed to operate up to a temperature of 315 °C and a pressure of 14 MPa. From the use of the laboratory- derived data, a method is presented whereby the viscosity of geothermal brine may be estimated from knowledge of its composition. To quantitative describe the thermodynamic and transport properties of geothermal fluids as a function of T, P, and x, the thermodynamic model (equation of state) or reference correlation model for transport properties are needed. Unfortunately, as was mentioned above, due to complexity physical chemical nature of the geothermal fluids, theory cannot accurately predict their thermodynamic properties needed for geothermal processes applications. The thermodynamic properties data for natural geothermal fluids are often missing and no equation of state for multicomponent aqueous salt solutions that valid in the wide T, P and x ranges. Inconsistence between existing theoretical models (equation of state) and experimental thermodynamic data for geothermal fluids is the result in difference and uncertainty in geochemical modeling.

The purpose of this study was to measure the density, speed of sound, and dynamic viscosity of four natural geothermal brines from Geothermal Filed of Dagestan (south Russia, Caspian seashore) and the effect of elevated temperatures (from 277 to 353 K) on these properties at various levels of dissolved ion concentrations. Another objective of the present study was to calculate other derived thermodynamic properties such as adiabatic coefficient of bulk compressibility, coefficient of thermal expansion, thermal pressure coefficient, isothermal coefficient of bulk compressibility, isochoric heat capacity, isobaric heat capacity, enthalpy difference, partial pressure derivative of enthalpy, and partial derivatives of internal energy (internal pressure) using the measured density and speed sound data. The correlation models for the density, viscosity, and speed of sound were also developed on bases of measured data. The in this work reported density, viscosity, and speed of sound data for the geothermal fluids at atmospheric pressure P_0 =0.101 MPa as a function of temperature were used as reference data to predict their high pressure behavior. In our recent publication (Abdulagatov et al., 2016) we have experimentally studied density, speed of sound, and viscosity of natural geothermal fluids from various geothermal wells with different chemical compositions. This paper reports the continuation of study on thermodynamic and transport properties natural geothermal fluids at atmospheric pressure and temperatures to 353 K. These data were used as a reference data for high pressure and high temperature prediction. The present results are considerably expanding the available data base on thermophysical properties of geothermal fluids from various regions of the South Russia Geothermal Fields with various chemical compositions. A major research goal of the future study is to develop thermodynamic models for the geothermal brines that can treat a wide range of T, P, and x.

2. GEOTHERMAL FIELD LOCATION AND WELLS CHARACTERISTICS

The geothermal fluid samples for the present study come from geothermal wells Izberbash (No.68 and 129), Thernair (No.27T and No.38T), located in south Russia Geothermal Field (Dagestan, Caspian seashore) (see Figs. 5). The Izberbash geothermal wells (No.68 and 129) are located approximately 38 miles to the south-west of capital city Makhachkala of Dagestan, near Caspian seashore (about 1 mile away from the seashore), at 42°32′ N & 47°53′ E. The Thernair wells (No.27T and No.38T) are located in the north-east part of the capital city Makhachkala (at 42°59′ N & 47°32′ E). The distance between the geothermal wells in Izberbash (No.68 and 129) and Thernair (No.27T and 38T) is about 40 miles. The wells (No.27T and No.38T) are closely located each other (the distance between them is about 1.25 miles), while distance between the wells (No.68 and 129) is about 0.6 miles. This region is commonly known for its rich natural surface geothermal springs (about 24 wells). This indicates that a larger scale hydrothermal hot source may existing the subsurface. The depths of the wells No.68, 129, 27T, and 38T are 1330, 1261, 2103, and 2060 m, respectively. All wells acting in continuously run regime since 1967. The wells characteristics are given in Table 1. The wellhead temperature T_{wh} is within (52 to 110) °C, while the wellhead pressure is from (0.06 to 0.64) MPa. The hot geothermal brines produced from the wells have the potential for possible district-usage applications for surrounding communities.

3. THE SAMPLES DESCRIPTION. CHEMICAL COMPOSITION OF THE GEOTHERMAL FLUID SAMPLES

Geothermal fluid is a brine solution as a result of it natural moving through the crust of the Earth. Geothermal fluids are responsible for mobility and transport of inorganic and organic solid and liquid phases and gaseous nonelectrolytes (Ague, 2003). The chemical composition of geothermal fluids varies widely between and within geothermal fields, and in some cases, over time within the same geothermal well. The exact chemical makeup of the geothermal fluids can have significant implications for both the design and operation of a geothermal plant and its potential environmental impact. The composition of a particular well varies as a function of the total production time, the rate of flow, and the nature of the underlying sediments. Thus, the brine compositions will vary from well to well, depending on the depth of production and the temperature of the different parts of the reservoir (Helgeson, 1967).

Figure 5: Geographical location of the geothermal area of Dagestan, (South Russia, near Caspian seashore) where the geothermal fluid sample comes from.

Table 1: Characteristics of the geothermal wells[a]

Well (No.)	Geological age	Date Drilled	Depth (m)	Production horizon/Perforated interval	Q (m^3/h)	P_{wh} (MPa)	T_{wh} (°C)
68	N_1ch	1967	1330	Chokrat /B	46	0.35	62
129	N_1ch	1979	1291	Chokrat /B	13	0.06	52
27T	N_1ch	1997	2103	Chokrat /B_2	104	0.90	98
38T	N_1ch	1985	2060	Chokrat /B_3	104	0.64	100

[a]Q, wellhead brine flow rate; T_{wh}, wellhead temperature; P_{wh}, wellhead temperature

Table 2: Chemical composition of geothermal brines from Izberbash and Thernair geothermal wells

Species	Sample: No.68 pH=7.2 *(mg/l)*	Sample: No.129 pH=7.2 *(mg/l)*	Sample: No. 27T pH=8.2 *(mg/l)*	Sample: No. 38T pH=7.7 *(mg/l)*
Cations				
All	<0.1	<0.1	<0.1	<0.1
As	<0.1	<0.1	<0.1	<0.1
B	1.2	2.4	59.3	59.8
Ba	<0.1	<0,1	1.7	2.0
Ca	49.2	2.8	73.6	72.6
Cd	<0.1	<0.1	<0.1	<0.1
Co	<0.1	<0.1	<0.1	<0.1
Cr	<0.1	<0.1	<0.1	<0.1
Cu	<0.1	<0.1	<0.1	<0.1
Fe	< 0.1	< 0.1	< 0.1	< 0.1
Hg	<0.1	<0.1	<0.1	<0.1
K	10.2	4.7	145	138
Li	0.2	0.1	2.2	2.1
Mg	32.9	1.3	28.5	29.6
Mn	<0.1	<0.1	<0.1	<0.1
Mo	<0.1	<0.1	<0.1	<0.1
Na	396	590	7540	7660
Ni	<0.1	<0.1	<0.1	<0.1
P	<0.1	0.2	<0.1	<0.1
Pb	<0.1	<0.1	<0.1	<0.1
S	240	211	39.8	34.2
Sb	<0.1	<0.1	<0.1	<0.1
Se	2.4	0.2	<0.1	<0.1
Si	13.8	12.3	29.4	28.1

Sr	1.1	0.1	6.7	6.8
Ti	<0.1	<0.1	<0.1	<0.1
Tl	<0.1	<0.1	<0.1	<0.1
V	<0.1	<0.1	<0.1	<0.1
Zn	<0.1	<0.1	<0.1	<0.1
Anions				
Chloride	152	176	7387	7689
Nitrate	<0.1	<0.1	<0.1	59.3
Sulfate	749	616	30.7	24.6
Total dissolved salt	1662.7	1830.0	15345.9	15808.0

Table 3: Mass percentage contents of main ions in the geothermal samples

Species	Sample: No.68 (%)	Sample: No.129 (%)	Sample: No.27T (%)	Sample: No.38T (%)
Sulfate	45.05	33.66	0.20	0.16
Sodium	23.82	32.24	49.13	48.46
Sulfur	14.43	11.53	0.26	0.22
Chlorine	9.14	9.62	48.14	48.64
Calcium	2.96	0.15	0.48	0.46
Magnesium	1.98	0.07	0.19	0.19
Silicon	0.83	0.67	0.19	0.18
Potassium	0.61	0.26	0.95	0.87
Boron	0.07	0.13	0.39	0.38
Other	<1.11	<11.67	<0.07	<0.44

Therefore, the properties of the geothermal fluids from various wells also are varying. The major chemical constituents of the geothermal samples include sodium (Na), chloride (Cl), bicarbonate (HCO_3), sulfate (SO_4), silica (SiO_2), calcium (Ca), and potassium (K). The chemical compositions of the brine samples taken from the Izberbash (No.68 and 129) and Thernair (No.27T and 38T) wells are presented in Table 2. An IRIS Intrepid II Optical Emission Spectrometer and Ion Chromatograph techniques were used to quantitative determination of the elemental composition (cations and anions) in the geothermal brine samples. The accuracy of the chemical composition measurements was 0.2% to 1.0%. As one can see from Table 2 the mineralization (total salt content) of the geothermal fluid samples from the wells No.68, 129, 27T, and 38T are 1.65 g/*l*, 1.62 g/*l*, 15.35 g/*l*, and 15.81 g/*l*, respectively, *i.e.*, both (No.68 and 129) and (No.27T and 38T) have almost the same concentrations. The main components of the geothermal samples are (see Table 3) sulfate (45.4%), sodium (24 %), sulfur (about 14.6%), chloride (9.2%), sodium (49.1%), and chlorine (48.1%). Although total mineralization of the samples (No.68 and 129) is very close (about 1.63 g/*l*), the percentage contents of the various ions in the samples are completely different. For example, sample No.68 contains 49.2 mg/*l* Ca^{+2} and 32.9 mg/*l* Mg^{+2}, while the contents of these ions in the sample No.129 are about 2.3 mg/*l* and 1.3 mg/*l*, respectively (both wells located very close each other).

The mineralogical compositions of the samples from No.27T and 38T are also very close each other (see Tables 2 and 3). Large difference in chemical compositions of the samples from wells (No.68, 129) and (No.27T, 38T) was observed (see Table 2). For example, as Table 2 shows, K^+ content in the sample (No.27T) is almost 31 times higher than in the sample (No.129), while Na^+ content in the sample (No.38T) 19.3 times higher than in the sample (No.68). The difference in Cl^{-1}, S^+, and B^+ content between the wells are within 44, 30, and 59 times, respectively. The wells (No.68 and 129) are located about 40 miles southern of (No 27T, 38T). The pH values for the geothermal fluids from various regions are roughly normally distributed around a median of 7.3, with the majority of values are between 5 and 10. For the present geothermal fluids the pH are 8.2 and 7.7 for samples (No.27T and 38T), respectively and 7.2 for samples (No.68 and 129). The major mineral components in the samples (No.68 and 129, both wells located very close to each other, about 0.6 mile) are (Na^+, SO^{-2}, Cl^{-1}, and Ca^{+2}), while for (No.27T and 38T, these wells located very close to each other, 1.25 miles) are (Na^+, K^{+1}, Ca^{+2} and Cl^{-1}).

Beside the dissolved solids, geothermal fluids contain some amount of dissolved gases (mostly N_2, CH_4, CO_2). The presence of the dissolved gases in geothermal fluids considerable influencing the thermodynamic properties, therefore, energy extraction processes. Due to pressure difference between the underground and the above ground (near surface, geothermal operations at 0.101 MPa) facility condition, degassing occurs during production. The average amount of dissolved gases in the geothermal fluid samples above ground (near surface, on the top of wells) are: 2.5 m^3 (gas) /m^3 (brine) for (No.27T), and 4.2 m^3 (gas) /m^3 (brine) for (No.38T). About (90 to 92) volume % gas content in the samples (No.27T and 38T) is hydrocarbon gases, while in the samples (No. 68 and 129) N_2 content is about (95 to 98) %.

Carbon dioxide content in the samples (No. 68 and 129) is (4 to 5) %, while in the samples (No.27T and 38T) is about (4.6 to 6.8) %. The contents of nitrogen and other rare gases in the samples from (No.27T and 38T) are about (2.6 to 3.3) %. When the composition, temperature and pressure of the geothermal brine in the geological formation are changing, (during reservoir evolution, well production, energy extraction or injection processes), the fluids that were originally at formation condition come to a new *P*, *T*, and *x* conditions. As a result, some solid minerals can precipitate, dissolved gases released and heat lost. Almost all geothermal energy operations experience these phenomena. The geothermal brine samples were collected at about (52 to 110) °C, filtered to remove suspended solids. No salts precipitations were observed during the samples collecting and low temperature (at 277 K) measurements.

4. EXPERIMENTAL

The method (experimental details, the physical basis and theory of the method, procedures, uncertainty assessment) and apparatus have been described in our recent publication (Abdulagatov et al., 2016). Only a brief review and essential information will be briefly given here.

4.1. Density measurements

The densities of the natural geothermal fluids were measured as a function of temperature with three different Anton Paar commercial instruments (DMA 4500, SVM 3000, and DSA 5000M). The digital density analyzer in these instruments uses a U-shaped vibrating tube (VTD). The working principle of an oscillation-type densimeter is based on the law of harmonic oscillation, in which a U-tube is completely filled with the sample under study and subjected to an electromagnetic force. Density measurements with a VTD are based on the dependence of the period of oscillation of a unilaterally fixed U-tube on its mass.

The calibration procedure with a minimum of two reference fluids such as water, air, nitrogen, benzene, and toluene whose *PVT* properties are well-known (Lemmon et al., 2010) were used to determine the temperature dependence of the calibration parameters in the working equation. The temperature in the measuring cell, where located the U-tube, was controlled using a thermostat with an uncertainty (k=2 and α=95% confidence level) of 10 mK and measured using the (ITS-90) PRT100 thermometer with an uncertainty 0.03 K over the range from (15 to 100) °C.

The densimeter (DMA4500) allows for a highly precise density measurements in the wide measuring range from (0 to 3000) kg·m^{-3} and at temperatures from (273 to 363) K. The uncertainty of the density measurements is 0.5 kg·m^{-3} (or about 0.05%). The repeatability of density and temperature measurements are 0.01 kg·m^{-3} and 0.01 K, respectively. This VTD has been successfully used previously in our earlier publications to accurate measure of the density of various fluids (see also Schmidt et al., 2012). The correction related with influence of the viscosity of the samples is within (0.001 to 0.004) %. The total absolute uncertainty (kg·m^{-3}) in density measurements caused by the viscosity effect can be approximately estimated as $\Delta\rho_b \approx 0.005\sqrt{\eta}$, where η is the viscosity of fluid in mPa·s. The correction for the present geothermal fluid samples is within from (0.03 to 0.06) kg·m^{-3}or (0.0035 to 0.006) %. Therefore, after correction the final uncertainty of the measured densities (including correction on the viscosity effect) is (0.503 to 0.506) kg·m^{-3} (or about 0.054 to 0.056%).

4.2. Viscosity measurements

The dynamic viscosity of the natural geothermal fluids at atmospheric pressure were measured with an automated SVM 3000 Anton Paar rotational Stabinger viscodensimeter with a coaxial cylinder geometry. The SVM 3000 viscodensimeter simultaneously measures the dynamic viscosity and density of liquids according to the ASTN D7042 standard. The technique allows simultaneously density (ρ), dynamic (η), and kinematic viscosity ($\nu = \eta/\rho$) measurements over the range (217 K to 378) K, and in the viscosity range of 0.2 mPa·s to 20 Pa·s. The details of the method widely described in the literature (Kroger, 2002/2003; Kratky et al., 1969, 1980; Stabinger et al., 1967; Stabinger, 1994; Leopold, 1970). The SVM3000 viscodensimeter uses Peltier elements for fast and efficient thermostability. The temperature uncertainty is 0.03 K. The precision of the dynamic viscosity measurements is ± 0.5% (stated by the manufacturer uncertainty is 0.35 %) and the absolute uncertainty of the density is 0.5 kg·m^{-3}. Repeatability of the viscosity and density are 0.2% and 0.2 kg·m^{-3}, respectively. Further details about the equipment and method can be found elsewhere (see, for example, Tariq et al., 2011; Carvalho et al., 2010).

4.3. Speed of sound measurements

The speed of sound of the geofluids at atmospheric pressure was measured with a sound-speed analyzer DSA 5000 M (Anton Paar instrument). DSA 5000 M simultaneously determines the density of the sample. The density and speed of sound measuring ranges are from (0 to 3000) kg·m^{-3} and from (1000 to 2000) m·s^{-1}, respectively. The uncertainties of the density and speed of sound measurements are 0.01% and 0.10%, with repeatabilities of 0.001 kg·m^{-3} and 0.10 m·s^{-1}, respectively. Combining of the density and speed of sound measurements in the DSA 5000 instruments makes it possible to determine the adiabatic compressibility (see below, sec. 5.3), $\beta_S = \frac{1}{W^2\rho}$. The two-in-one instrument is equipped with a density cell and a sound velocity cell thus combining the proven Anton Paar oscillating U-tube method (see above sec. 4.1) with a highly accurate measurement of sound velocity. Both cells are temperature-controlled by a built-in Peltier thermostat. The sample is introduced into the sound velocity-measuring cell that is bordered by an ultrasonic transmitter on the one side, by a receiver on the other side. The transmitter sends sound waves of a known period through the sample. The speed of sound can be calculated by determining of the period of received sound waves and by considering the distance between the transmitter and receiver.

5. RESULTS AND DISCUSSION

Measurements of the density, speed of sound, and viscosity of the geothermal fluid samples from four hot-wells (No.68, 129, 27T and 38T) as a function of temperature at atmospheric pressure were performed at temperatures between (277 and 353) K. The experimental density, viscosity, and speed of sound results are presented in Table 4 and shown in Figs. 1-4 as a function of temperature together with pure water values calculated from the IAPWS formulations for the density (Wagner and Pruß, 2002) and viscosity (Huber et al., 2009). The measurements of the density of geothermal fluids (the same samples) were made using three different Anton Paar instruments of DMA 4500, SVM 3000, and DSA 5000M (vibrating-tube densimeter, VTD). The measured data from different instruments agree with

each other within (0.01 to 0.02) % which is close to their experimental uncertainties. In general, the qualitative behavior of the present measured density, viscosity, and speed of sound data for all of the studied geothermal brines very close to temperature behavior of pure water (see Figs. 1-4). The same behavior has been observed also for reported data of binary and ternary aqueous salt solutions (see, for example, Abdulagatov et al. 2005a-c, 2007; Abdulagatov and Azizov 2006; Abdulagatov and Assael, 2009). In the present study we found that at low temperatures the deviation of the solution viscosity data from the water data is slightly lower than at high temperatures, especially for high salt concentrations samples. However, this is still within experimental uncertainty of the viscosity measurements. In the measured temperature range (from 277 to 353 K) the average difference between the present measured geothermal fluids densities and pure water values (Wagner and Pruß, 2002) are No.68: (0.05to 0.10) %; No.129: (0.15 to 0.21)%; No.27T: (1.47 to 1.64) %; and for No.38T: (1.54 to 1.77) %, which are considerably higher than their experimental uncertainties, especially for wells 27T and 38T which mineralizations are large (almost 10 times higher than for wells No.68 and 129). As one can see from Figs. 1-4 the measured values of properties (density, speed of sound, and viscosity) for samples from wells No.68 and 129 are very close each other. The same results we found for the samples No.27T and 38T. It is obviously, because the difference between the compositions of the samples from wells No. 68 and 129 (both very closely located, 0.6 miles) is small (total salt contents are 1.7 and 1.8 g/*l*, respectively, see also Tables 2 and 3). Also the location of the wells No.27T and 38T is very close (1.25 miles) and the composition of the samples from the wells is very close (15.4 and 15.8 g/*l*, respectively, see also Tables 2 and 3). However, the difference of the salt concentrations between the samples from wells (No.68, 129) and (No.27, 38T) is considerable large. Thus, the property differences between the samples from (No.68, 129) and (No.27, 38T) are very large (see below).

The present viscosity data for the geothermal brines are differing from those of pure water by (1.3 to 13.1) % for No.68; by (0.6 to 4.8)% for No.129; by (5.6 to 19.5)% for No.27T; and by (3.1 to 21.0)% for No.38T, which are considerably higher than their experimental uncertainty. The measured speed of sound data for geothermal fluids is differing from pure water values (Wagner and Pruß, 2002) within (0.13 to 0.25) % for No.68; by (0.3 to 2.1) % for No.129; by (1.33 to 1.97) % for No.27T; and by (1.37 to 2.04) % for No.38T, which are also much higher than the experimental uncertainty. Viscosity is more sensitive properties to salt concentration than thermodynamic properties (density and speed of sound). As one can be note, measured properties for geothermal fluids (No.27T and 38T) are considerably (up to 1.77% for density, 21% for the viscosity, and 2.04% for speed of sound) deviate from the values for pure water than for geothermal samples from (No.68 and 129). This is the result of the large composition difference between the samples (No.27T and 38T, mineralization is about 15.5 g/*l*) and samples (No.68 and 129, mineralization of 1.8 g/*l*). However, this effect depends not only on the total concentration of ions, but also on chemical nature of the ions, *i.e.*, type of chemical ion species in the brine. For example, the samples (No.68 and 129 from the same Geothermal Fields, Izberbash) have almost the same mineralization of about 1.75 g/*l*), however concentration contents of ions (for example, Ca^{+2}, K^{+1}, Mg^{+2}, and Na^{+1} in the sample No.68 are 49.2, 10.2, 33, and 396 mg/*l*), while the content of the same ions in the sample No.129 are completely different 2.8, 4.7, 1.3, and 590 mg/*l*, respectively). Therefore, the properties of the samples No.68 and 129 are also different. This is demonstrating how the chemical nature of the ion species is effecting on the measuring properties. Separation of the contribution of single ion species to the total measured properties in the multicomponent geothermal solutions is difficult, because the solution properties are defining not only by interaction between the water molecules and single ions, but also between the ion-ion interactions, which made the problem more complicate. The presence of various type ions in the solution considerable changes the effect of particular type ions on their properties. Therefore, prediction of the thermophysical properties of multicomponent aqueous solutions, like geothermal brine, based on empirical method and solely on reliable experimental data. Thus, the present experimental data for geothermal fluids can be used to develop new prediction methods and to test the available prediction techniques.

The distinct density, speed of sound, and viscosity contributions (single ion species contributions) to the total measured properties of the multicomponent geothermal solutions, can be separated and extracted from the present measured total thermophysical properties data. The measured properties are complex functions of temperature. The temperature dependence of the density, speed of sound, and viscosity is determined by many different contributions of ion species. The present accurate measurements of the temperature dependence of the total density, speed of sound, and viscosity for various geothermal fluid samples with various salt concentrations allow correctly estimate the contribution of each single ion species and deeply understanding the physical and chemical nature and details of the temperature and concentration dependences of the measured properties (see below sec.5.1).

5.1. Correlation models for density, viscosity, and speed of sound

Since there is no theory available for the thermodynamic (equation of state) and transport properties (temperature and concentration dependence correlation models) of multicomponent aqueous solutions, its evaluation is empirical and based solely on experimentally obtained data. Therefore, the present density, speed of sound, and viscosity data for the geothermal fluid samples were fitted to the correlation equations

$$\rho(T,x_i)=\rho_{H_20}(T)\left(1+\sum_{i=1}^{n}a_i x_i\right), \tag{1}$$

$$W(T,x_i)=W_{H_20}(T)\left(1+\sum_{i=1}^{n}c_i x_i\right), \tag{2}$$

$$\eta(T,x_i)=\eta_{H_20}(T)\left(1+\sum_{i=1}^{n}b_i x_i\right), \tag{3}$$

where $\rho_{H_20}(T)$, $W_{H_20}(T)$, and $\eta_{H_20}(T)$ are the pure water density, speed of sound (IAPWS formulation, Wagner and Pruß, 2002), and viscosity (IAPWS formulation, Huber et al., 2009), respectively at a temperature T and at atmospheric pressure; xi is the concentration of ions (g/l); n is the number of main components (n=9); ai, bi, and ci are the density, viscosity, and speed of sound coefficients (characteristic constant of the ions) for each ion species i. It is apparent that the empirical parameters ai, bi, and ci are defined the contribution of each single ion species to total measured properties and allow separate the contribution of different species. For the present geothermal fluid samples we selected 6 main components (ions): Na+, Ca+2, Mg+2, K+, SO_4^{-2}, and Cl^{-1}. The effect of other ions on the measured properties is negligible small. Since the thermodynamic behavior of the geothermal fluids (binary and ternary aqueous salt solutions) governs by the properties of pure water (see Figs. 1-4), the temperature is not explicitly included in correlations (1) to (3), i.e., the temperature dependence of the measured properties is determined through the pure water properties. All of the measured density, speed of sound, and viscosity data from Table 4 for the geothermal fluids together with the ions concentrations from Table 2 were fitted to Eqs. (1)-(3). The derived values of fitting parameters a_i, b_i, and c_i are given in Table 5. The values of characteristic constant of the ions, a_i, b_i, and, and ci, (or Riedel's characteristic constant of the ions) defined the contribution of each type ions on the total experimentally observed values of density, viscosity, and speed of sound. Riedel (1951), Aseyev and Zaytsev (1996), and Aseyev (1998) have proposed the same correlation model for the thermal conductivity and other thermophysical properties of multicomponent aqueous salt solutions. This relation for the thermal conductivity gives good prediction agreement (within 5 %) with the experimental data for many aqueous salt solutions (Abdulagatov et al. 2005a; Abdulagatov and Assael, 2009). Many authors checked the accuracy and predictive capability of the Riedel's model (see also review by Horvath, 1985; Abdulagatov et al., 2005; and Abdulagatov et al., 2016). The deviation statistics between the measured and calculated values for density, speed of sound, and viscosity are given in Table 6. As Table 6 shows, these correlation Eqs. (1)-(3) reproduced the present density, speed of sound, and viscosity measurements for the geothermal brines within AAD=0.03%, 0.20%, and 2.47%, respectively. The values of density, speed of sound, and viscosity calculated from Eqs. (1)-(3) together with the present measured results are presented in Figs. 1-4. To confirm the accuracy and reliability of the developed correlation models (1) to (3), we have compared the predicted values of the density and viscosity with the reported data for well-studied binary aqueous salt solutions. For example, the difference between the measured values of viscosity by Kestin and Shankland (1984) and speed of sound data by Golabiazar and Sadeghi (2014) and the present results calculated from Eqs. (2) and (3) for H2O+NaCl solution are within 1.56 % and 0.2 %, respectively (see Figs. 3 and 6).

Developed correlation equations (1)-(3) can be used to calculate the density, speed of sound, and viscosity of any geothermal fluids at atmospheric pressure with basic components of Na+, Ca+2, K+1, Mg+2, B+1, S+1, Si+1, SO_4^{-2}, Cl^{-1} and with concentrations within $x(Na^+)$<7.7 g/l; $x(Ca^+)$<0.075 g/l; $x(Mg^+)$<0.033 g/l; $x(K^+)$<0.015 g/l; $x(S^+)$<0.24 g/l; $x(B^+)$<0.06 g/l; $x(Si^+)$<0.03 g/l; $x(SO_4^{-2})$<0.75 g/l; and $x(Cl^{-1})$<7.7 g/l.

It is apparent that these correlation models cannot be used for geothermal fluid samples with the concentration of salt ions outside the experimental concentration ranges (see Table 2). More measurements for geothermal brines from various geothermal fields with various compositions are needed to develop accurate prediction models applicable for any natural geothermal fluids with a wide range of composition of salt ions. In order to extend the concentration and temperature ranges where the models (1) to (3) are valid and improve the accuracy of the experimental data representations, the next terms ($x_i^{0.5}$, x_i, $x_i^{1.5}$, x_i^2) in expansion Eqs. (1)-(3) can be used.

Table 4: Experimental values of density, viscosity, and speed of sound as a function of temperature for geothermal fluids at atmospheric pressure[c]

Izberbash (No.68)

T (K)	ρ[a] (kg·m^{-3})	T (K)	ρ[b] (kg·m^{-3})	η[b] (mPa·s)	T (K)	ρ[c] (kg·m^{-3})	W[c] (m·s^{-1})
277.16	1000.97	277.15	1000.78	1.588	278.15	1000.72	1429.79
283.16	1000.65	283.15	1000.55	1.328	283.15	1000.51	1450.32
293.17	999.00	293.15	999.01	1.032	293.15	998.91	1484.84
303.13	996.42	303.15	996.40	0.835	303.15	996.43	1511.31
313.13	992.94	313.15	992.92	0.700	313.15	992.91	1530.94
323.13	988.73	323.15	988.70	0.603	323.15	988.72	1544.64
		333.15	983.69	0.536	333.15	983.72	1553.12

Izberbash (No.129)

T (K)	ρ[a] (kg·m^{-3})	T (K)	ρ[b] (kg·m^{-3})	η[b] (mPa·s)	T (K)	ρ[c] (kg·m^{-3})	W[c] (m·s^{-1})
277.17	1002.02	277.15	1002.04	1.576	278.13	1002.01	1430.42
283.15	1001.71	283.15	1001.69	1.339	283.15	1001.74	1451.31

293.16	1000.13	293.15	1000.17	1.048	293.15	1000.10	1486.27
303.13	997.56	303.15	997.55	0.816	303.15	997.79	1512.68
313.13	994.10	313.15	994.05	0.676	313.15	994.02	1532.20
323.13	989.83	323.15	989.80	0.568	318.15	992.07	1539.74
		333.15	984.60	0.488	323.15	989.76	1545.85
		343.15	979.17	0.421	333.15	984.64	1553.97
		353.15	973.39	0.372			

Thernair (No.27T)

T (K)	ρ^{a} (kg·m^{-3})	T (K)	ρ^{b} (kg·m^{-3})	η^{b} (mPa·s)	T (K)	ρ^{c} (kg·m^{-3})	W^{c} (m·s^{-1})
277.17	1016.60	277.15	1016.4	1.660	278.14	1016.50	1456.68
283.17	1015.82	283.15	1015.87	1.420	283.15	1015.89	1476.34
293.17	1013.75	293.15	1013.73	1.119	293.14	1013.70	1508.65
303.13	1010.80	303.15	1010.78	0.917	303.15	1010.76	1533.06
313.13	1007.06	313.15	1007.03	0.785	313.15	1007.01	1551.46
323.13	1002.84	323.15	1002.81	0.679	323.10	1002.70	1564.20
					333.15	997.98	1571.92

Thernair (No.38T)

T (K)	ρ^{a} (kg·m^{-3})	T (K)	ρ^{b} (kg·m^{-3})	η^{b} (mPa·s)	T (K)	ρ^{c} (kg·m^{-3})	W^{c} (m·s^{-1})
277.16	1017.00	277.15	1017.08	1.618	278.14	1016.82	1455.79
283.17	1016.03	283.15	1016.05	1.373	283.15	1016.03	1475.53
293.16	1014.34	293.14	1014.38	1.089	293.15	1014.36	1507.58
303.13	1011.45	303.15	1011.43	0.885	303.15	1011.47	1532.40
313.13	1007.77	313.15	1007.73	0.756	313.15	1007.80	1550.72
-	-	323.15	1003.45	0.648	318.15	1005.85	1558.02
-	-	333.15	998.65	0.570	323.15	1003.50	1563.40
-	-	343.15	993.47	0.516	-	-	-

[a]DMA4500;

[b]SVM3000;

[c]DSA 5000M; Standard uncertainties u are: (DMA4500) $u(T)$=0.01K; $u(\rho)$=0.00025 %; (SVM3000) $u(T)$=0.005K; $u(\rho)$=0.01 %; $u(\eta)$=0.17 %; (DSA 5000M) $u(\rho)$=0.005 % (or 0.002 kg·m^{-3}); $u(W)$=0.005 % (or 0.05 m·s^{-1}).

Table 5: Values of fitting coefficients a_i, b_i, and c_i for density, viscosity, and speed of sound correlation models Eqs. (1)-(3) for basic ions in the geothermal fluid samples (density)

Ions	a_i (density) (l/g)	b_i (viscosity) (l/g)	c_i (speed of sound) (l/g)
B^{+}	-0.385842	0.539016	-0.418696
Ca^{+2}	0.025925	-0.716700	0.066130
K^{+}	-0.005234	-0.986039	0.044718
Mg^{+2}	-0.046190	1.444916	-0.105018
Na^{+}	0.006454	0.017450	0.006028
S^{+}	0.006349	0.028139	0.008064
Si^{+}	-0.223142	-2.751235	-0.084065
Cl^{-1}	-0.000498	0.020534	-0.001379
SO_4^{-2}	0.000784	0.067295	-0.001405

Table 6: Deviation statistics between the measured and calculated from Eqs. (1)-(3) values of density, speed of sound, and viscosity

Deviations	Density	Speed of sound	Viscosity
AAD (%)	0.03	0.20	2.47
Bias (%)	-0.01	0.15	0.71
St.dev (%)	0.04	0.22	3.16
St.err (%)	0.01	0.06	0.65
Maxdev (%)	0.16	0.50	6.92

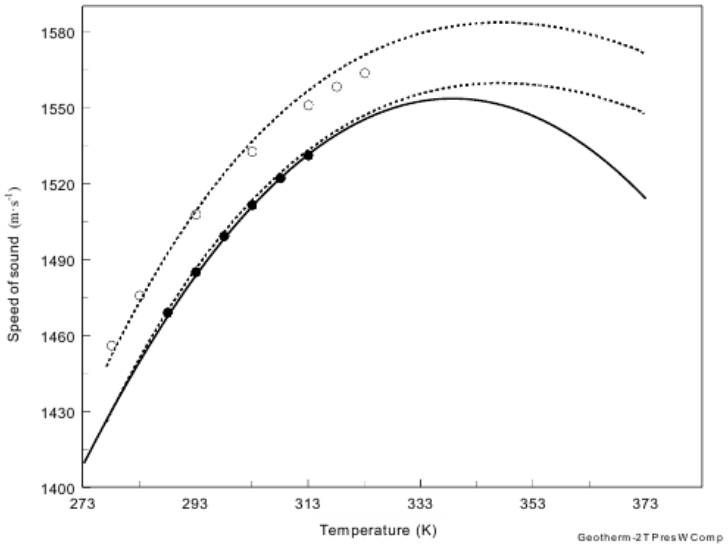

Figure 6: Calculated from Eqs. (2) and (7) values of speed of sound for geothermal fluids (No:68, full circles) and (No.38T, open circles) together with the reported data by Golabiazar and Sadeghi (2014) for H_2O+NaCl at atmospheric pressure. Dashed lines are predicted from Eq. (7). Solid line is calculate from Eq. (2). ○- this work for geothermal fluid sample No. 38T; ●-reported data by Golabiazar and Sadeghi (2014) for H_2O+NaCl.

5.2. High pressure prediction models

DiGuilio et al. (1990) and DiGuilio and Teja (1992) proposed empirical predictive equation for high pressure behavior of the thermal conductivity of aqueous salt solutions by multiplying the thermal conductivity of the salt solution at reference pressure, P_0 (usually at P_0 =0.101 MPa) and any temperature T, by the ratio of the thermal conductivity of pure water at the desired pressure P to that at a known (reference) pressure, P_0 =0.101 MPa at the same temperature T. If the viscosity or other thermophysical properties (density, speed of sound, thermal conductivity, *etc.*) of the salt solution (or geothermal fluids) are known at the reference pressure (for example, P_0 =0.101 MPa) and any temperature T, the properties at any pressures (at which the property of pure water is known) may be calculated as

$$\rho(P,T,x_i)=\rho(P_0,T,x_i)\left(\frac{\rho_{H_2O}(P,T)}{\rho_{H_2O}(P_0,T)}\right)_{H_2O}, \tag{4}$$

$$\eta(P,T,x_i)=\eta(P_0,T,x_i)\left(\frac{\eta_{H_2O}(P,T)}{\eta_{H_2O}(P_0,T)}\right)_{H_2O}, \tag{5}$$

$$W(P,T,x_i)=W(P_0,T,x_i)\left(\frac{W_{H_2O}(P,T)}{W_{H_2O}(P_0,T)}\right)_{H_2O}, \tag{6}$$

where $\rho(P_0,T,x_i)$, $\eta(P_0,T,x_i)$ and $W(P_0,T,x_i)$ can be calculated from Eqs. (1)-(3) at P_0 =0.101 MPa based on the present data. The present measured values of the thermodynamic (density and speed of sound) and transport (viscosity) property of geothermal fluids at atmospheric pressure were used to predict their pressure dependences based on Eqs. (4)-(6). The predicted values of density, speed of sound, and viscosity for geothermal fluids as a function of pressure and temperature are presented in Figs. 7 and 8 for various isobars and isotherms. This technique has been successfully used before and tested by many authors (see for example, DiGuilio and Teja, 1992; DiGuilio et al.,1990; Abdulagatov et al.,2005a) to predict the thermal conductivity and other thermodynamic properties of different aqueous salt solutions at high pressures and high temperatures. The same approach to predict the high temperature behavior of the aqueous solutions properties (thermal conductivity) based on the room temperature data for the solution and high temperature pure water data was developed by Vargaftik and Osminin (1956) based on the relation

$$Y(P_0,T,x_i)=Y(P_0,T_0,x_i)\left(\frac{Y_{H_2O}(P_0,T)}{Y_{H_2O}(P_0,T_0)}\right)_{H_2O}, \tag{7}$$

where $Y(P_0,T,x_i)$ is the selected values of thermophysical properties (density, speed of sound, viscosity, thermal conductivity, *etc.*) of salt solution at atmospheric pressure. Application of the relation (7) for the present measured densities of geothermal fluid (#38T) are depicted in Fig. 9. As can be note, the agreement between the present measurements and the predicted values of density is good enough (deviation AAD within 0.12%). Difference between the predicted from Eq. (4) values of density for H_2O+NaCl at high pressures (at 20 MPa) and reported by Rogers and Pitzer (1982) data is within AAD=0.023% (see Fig.10). Difference between the predicted values of viscosity at high pressures and measurements by Kestin and Shankland (1984) for H_2O+NaCl is within (1-2)% (see Fig. 11). Fig. 11 demonstrate temperature dependence of viscosity of H_2O+NaCl solution calculated from Eq. (5) at selected pressures (10 and 20 MPa) using the present correlation model (3) together with the data by Kestin and Shankland (1984). This figure also shows pressure dependence of viscosity of the H_2O+NaCl solution for selected isotherms. The agreement is acceptable, although the measured values of viscosity are systematically lower than predicted values (above than the experimental uncertainty of 0.5%).

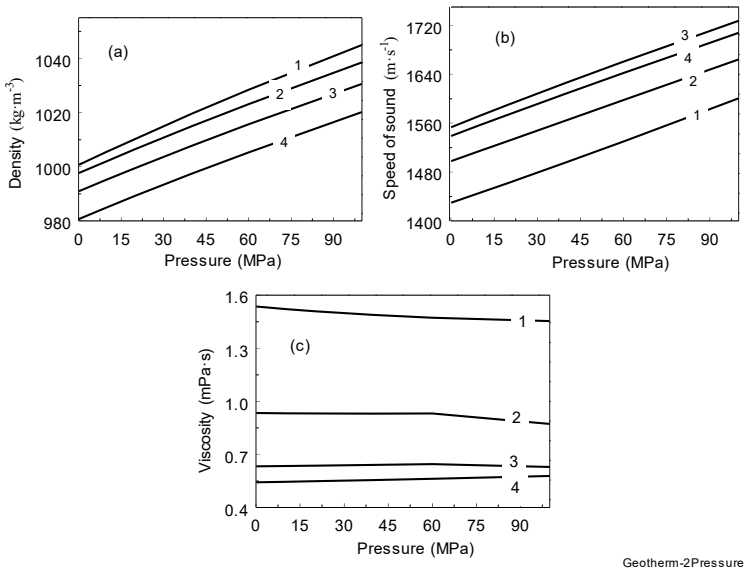

Figure 7: Predicted, from equations (4)-(6), values of density (a), speed of sound (b), and viscosity (c) as a function of pressure at selected isotherms for geothermal fluid sample of No.68. 1-278 K; 2-298 K; 3-318 K; 4-338 K.

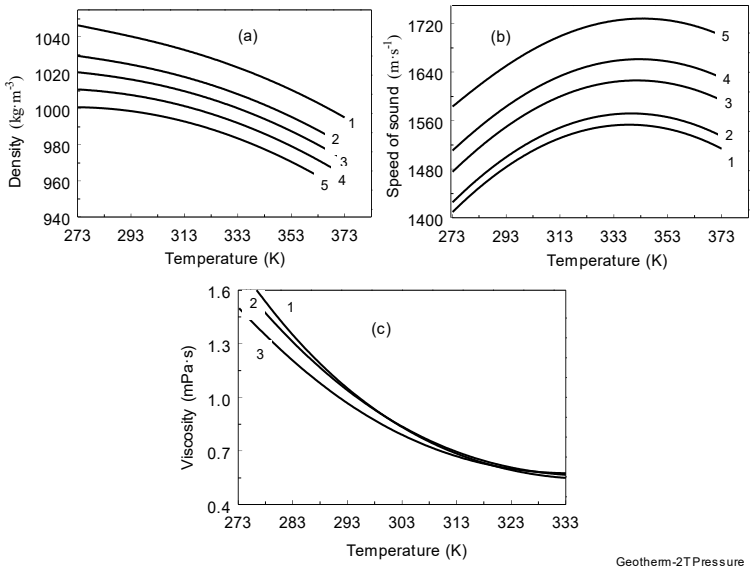

Figure 8: Predicted, from equations (4)-(6), values of density (a), speed of sound (b), and viscosity (c) as a function of temperature at selected isobars for geothermal fluid sample of No. 68. 1-0.101 MPa; 2-20 MPa; 3-40 MPa; 4-60 MPa; and 5-100 MPa.

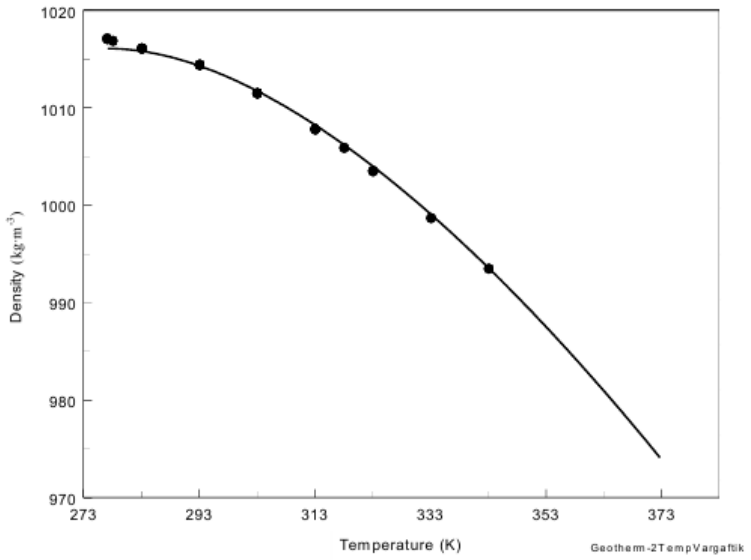

Figure 9: Measured and predicted from equation (7) values of density for geothermal fluid No.38T.

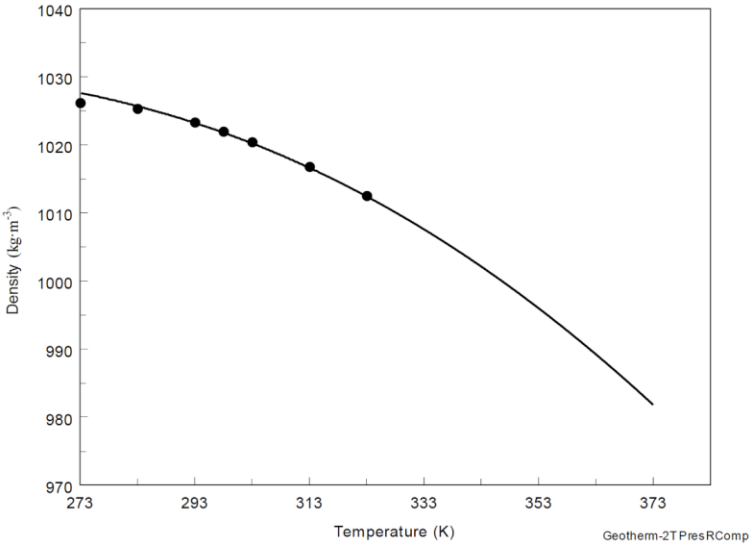

Figure 10: Comparison predicted from Eq. (4) values of density at high pressure (*P*=20 MPa) for geothermal fluids (No:38T) with the measured values for H_2O+NaCl solutions. Solid line is predicted from Eq. (4). Symbols are reported reference data by Rogers and Pitzer (1982).

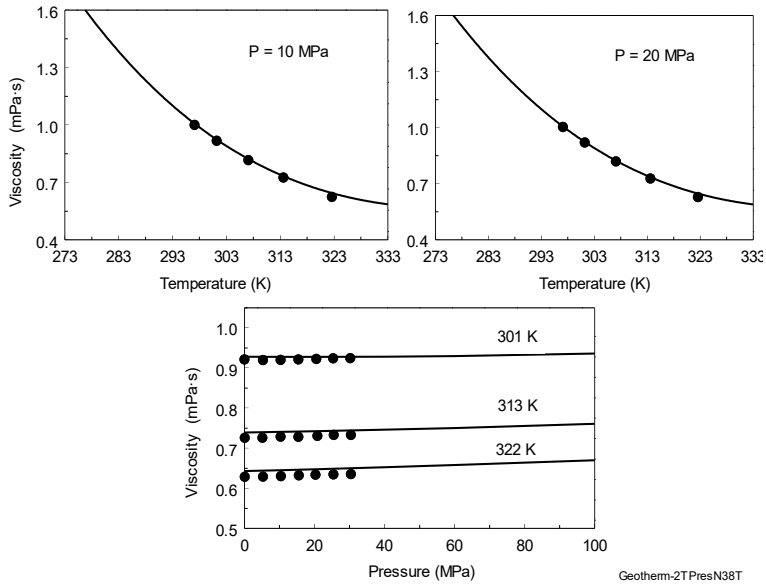

Figure 11: Comparison predicted from Eq. (5) values of viscosity at high pressures for geothermal fluid (No:38T) with measured values for H_2O+NaCl solutions by Kestin and Shankland (1984).

5.3. Derived thermodynamic properties of geothermal fluids

The measured values of density and speed of sound for the natural geothermal fluids were used to calculate other thermodynamic parameters such as, $\beta_S, \beta_T, \alpha_P, \gamma_V, \Delta H, C_P, C_V, \left(\frac{\partial H}{\partial P}\right)_T, \left(\frac{\partial U}{\partial V}\right)_T$. All of these thermodynamic properties were calculated using the well-known thermodynamic relations:

1. Adiabatic coefficient of bulk compressibility,

$$\beta_S = \frac{1}{W^2 \rho}; \tag{8}$$

where $\beta_S = -\frac{1}{V}\left(\frac{\partial V}{\partial P}\right)_S$ has been calculated using measured densities (ρ) and speed of sound data (W) from Table 4;

2. Coefficient of thermal expansion,

$$\alpha_P = -\frac{1}{\rho}\left(\frac{\partial \rho}{\partial T}\right)_P; \tag{9}$$

has been calculated using measured densities (ρ) as a function of temperature from Table 4;

3. Thermal pressure coefficient,

$$\gamma_V = \left(\frac{\partial P}{\partial T}\right)_V = \left(\frac{dP_S}{dT}\right) + \frac{1}{T}\frac{dT}{dV_S}\Delta C_V, \tag{10}$$

where ΔC_V is the one- and two-phase heat capacity difference, V_S is the specific volume at saturation, and P_S is the vapor pressure (Abdulagatov end Dvoryanchikov, 1995);

4. Isothermal coefficient of bulk compressibility,

$$\beta_T = \frac{\alpha_P}{\gamma_V}, \text{ where } \beta_T = -\frac{1}{V}\left(\frac{\partial V}{\partial P}\right)_T \tag{11}$$

5. Isochoric heat capacity,

$$C_V = VT\alpha_p\gamma_V / \left(W^2\rho\alpha_p/\gamma_V - 1\right), \text{ where } V = 1/\rho; \tag{12}$$

6. Isobaric heat capacity,

$$C_P = C_V W^2 \rho\alpha_p / \gamma_V; \tag{13}$$

7. Enthalpy difference,

$$\Delta H = H(T) - H(T_0) = \int_{T_0}^{T} C_P(T)dT, \tag{14}$$

has been calculated using derived C_P data;

8. Partial pressure derivative of enthalpy,

$$\left(\frac{\partial H}{\partial P}\right)_T = V\left(1 - T\alpha_P\right), \tag{15}$$

9. Partial derivatives of internal energy (internal pressure),

$$\left(\frac{\partial U}{\partial V}\right)_T = -P_0 + T\gamma_V, \text{ where } P_0 = 0.101 \text{ MPa} \tag{16}$$

Derived thermodynamic properties of geothermal fluids calculated using Eqs. (8)-(16) are given in Tables 7 and 8. Thus, in Table 4, 7, and 8 we have all of the thermodynamically consistent property data as a function of temperature at atmospheric pressure for four natural geothermal fluids. Unfortunately, there are no direct measured thermodynamic properties data for the present geothermal fluids to check the accuracy and reliability of the derived properties. However, this method of calculation of the thermodynamic properties has been checked for many other fluids (see for example, Abdulagatov et al., 2005a).

CONCLUSIONS

The density, speed of sound, and viscosity of four natural geothermal fluid samples from Dagestan Geothermal Field (south Russia, Caspian seashore) have been measured with Anton Paar Instruments: vibrating-tube densimeters (DMA 4500); sound-speed analyzer (DSA 5000 M); and Stabinger viscodensimeter (SVM3000), respectively. Measurements were made at temperatures from (277 to 353) K and at atmospheric pressure. The temperature behavior of the density, speed of sound, and viscosity for geothermal fluids are just like pure water and other binary and ternary aqueous salt solutions. The average differences between the measured geothermal fluids density, speed of sound, and viscosity and pure water values (IAPWS formulations, 2002 and 2009) are within (0.05 to 1.77)%, (0.13 to 2.04)%, and (0.6 to 21.0)%, respectively, which are much higher than their experimental uncertainties. The measured density, speed of sound, and viscosity data were used to develop correlation model (Riedel model) to predict the values of these properties for various concentrations of ions and temperatures from (277 to 353) K. The contribution (Riedel's characteristic constant of the ions) of the basic ions in the geothermal fluids (Ca^{+2}, K^{+1}, Mg^{+2}, Na^{+1}, B^{+1}, S^{+1}, Si^{+1}, SO^{-2}, and Cl^{-1}) to the total experimentally observed values of the density, viscosity, and speed of sound was estimated. The models reproduced measured values of density, speed of sound, and viscosity of geothermal fluids within: density: AAD=0.03%; speed of sound: AAD=0.20%; and viscosity: AAD=2.47%. It was shown that if the thermophysical properties of geothermal fluid are known at reference pressure (for example, P_0=0.101 MPa) and any temperature, their properties at any high pressures (at which this properties of pure water is known) and temperatures maybe calculated by multiplying the properties of the geothermal fluid at reference state, P_0, and given temperature, T, by the ratio of the this property of pure water at the desired pressure to that at a known reference pressure, P_0=0.101 MPa. The prediction of the values of density and viscosity from the model at high pressures for H_2O+NaCl solutions agree with the data reported by Rogers and Pitzer (1982) and Kestin and Shankland (1984) within AAD = 0.023% and 1.5%, respectively. The measured values of viscosity at high pressures are systematically lower than predicted values (slightly higher than the experimental uncertainty of 0.5%). The measured values of density and speed of sound were also used to calculate other derived properties such as adiabatic coefficient of bulk compressibility, coefficient of thermal expansion, thermal pressure coefficient, isothermal coefficient of bulk compressibility, isochoric heat capacity, isobaric heat capacity, enthalpy difference, partial pressure derivative of enthalpy, and partial derivatives of internal energy (internal pressure). More measurements for geothermal brines from various geothermal fields with various compositions are needed to develop accurate prediction models applicable for any natural geothermal fluids with wide range of composition of salt.

Table 7: Derived, from the present density and speed of sound measurements, values of thermodynamic properties of geothermal fluids

Izberbas (No. 68)

T (K)	$\beta_S \times 10^3$ (MPa^{-1})	$\alpha_P \times 10^3$ (K^{-1})	$\left(\frac{\partial H}{\partial P}\right)_T$ (cm^3·g^{-1})	$\left(\frac{\partial U}{\partial V}\right)_T$ (MPa)	$\beta_T \times 10^3$ (MPa^{-1})	γ_V (MPa·K^{-1})	C_V (kJ·kg^{-1}·K^{-1})	C_P (kJ·kg^{-1}·K^{-1})
278.15	0.4888	0.0637	0.9816	36.12	0.4891	0.130233	4.259	4.262
283.15	0.4752	0.1089	0.9687	64.68	0.4760	0.228790	4.217	4.224
293.15	0.4541	0.1996	0.9425	127.95	0.4569	0.436804	4.163	4.188
303.15	0.4394	0.2908	0.9151	197.73	0.4455	0.652591	4.121	4.179
313.15	0.4297	0.3828	0.8864	271.85	0.4408	0.868439	4.080	4.185
323.15	0.4239	0.4758	0.8559	348.14	0.4415	1.077650	4.031	4.198
333.15	0.4214	0.5702	0.8235	424.47	0.4474	1.274407	3.990	4.236

Izberbash (No. 129)

T (K)	$\beta_S \times 10^3$ (MPa^{-1})	$\alpha_P \times 10^3$ (K^{-1})	$\left(\frac{\partial H}{\partial P}\right)_T$ (cm^3·g^{-1})	$\left(\frac{\partial U}{\partial V}\right)_T$ (MPa)	$\beta_T \times 10^3$ (MPa^{-1})	γ_V (MPa·K^{-1})	C_V (kJ·kg^{-1}·K^{-1})	C_P (kJ·kg^{-1}·K^{-1})
278.13	0.4878	0.0964	0.9712	54.82	0.4884	0.197475	4.282	4.288
283.15	0.4739	0.1356	0.9600	80.73	0.4752	0.285460	4.257	4.268
293.15	0.4526	0.2140	0.9372	137.52	0.4558	0.469468	4.209	4.238
303.15	0.4380	0.2929	0.9132	199.77	0.4442	0.659320	4.163	4.222
313.15	0.4285	0.3724	0.8887	265.60	0.4389	0.848470	4.110	4.209
318.15	0.4252	0.4125	0.8757	299.44	0.4381	0.941522	4.092	4.217
323.15	0.4228	0.4528	0.8625	333.50	0.4387	1.032340	4.070	4.223
333.15	0.4206	0.5344	0.8348	401.43	0.4434	1.205260	4.020	4.238

Thernair (No. 27T)

T (K)	$\beta_S \times 10^3$ (MPa^{-1})	$\alpha_P \times 10^3$ (K^{-1})	$\left(\frac{\partial H}{\partial P}\right)_T$ (cm^3·g^{-1})	$\left(\frac{\partial U}{\partial V}\right)_T$ (MPa)	$\beta_T \times 10^3$ (MPa^{-1})	γ_V (MPa·K^{-1})	C_V (kJ·kg^{-1}·K^{-1})	C_P (kJ·kg^{-1}·K^{-1})
278.14	0.4636	0.1382	0.9460	82.58	0.4648	0.297274	4.288	4.299
283.15	0.4516	0.1740	0.9359	108.48	0.4536	0.383488	4.244	4.262
293.14	0.4334	0.2456	0.9155	164.42	0.4376	0.561219	4.190	4.230
303.15	0.4210	0.3178	0.8940	224.95	0.4282	0.742359	4.141	4.212
313.15	0.4126	0.3907	0.8715	288.61	0.4238	0.921960	4.105	4.217
323.10	0.4076	0.4641	0.8478	353.53	0.4240	1.094500	4.065	4.229
333.15	0.4055	0.5393	0.8220	419.24	0.4284	1.258700	4.012	4.239

Thernair (No. 38T)

T (K)	$\beta_S \times 10^3$ (MPa^{-1})	$\alpha_P \times 10^3$ (K^{-1})	$\left(\frac{\partial H}{\partial P}\right)_T$ (cm^3·g^{-1})	$\left(\frac{\partial U}{\partial V}\right)_T$ (MPa)	$\beta_T \times 10^3$ (MPa^{-1})	γ_V (MPa·K^{-1})	C_V (kJ·kg^{-1}·K^{-1})	C_P (kJ·kg^{-1}·K^{-1})
278.14	0.4640	0.1347	0.9466	80.42	0.4652	0.289510	4.307	4.318
283.15	0.4521	0.1692	0.9371	105.42	0.4539	0.372668	4.278	4.296
293.15	0.4338	0.2383	0.9170	159.51	0.4376	0.5444502	4.225	4.263
303.15	0.4210	0.3078	0.8964	218.08	0.4277	0.7197100	4.165	4.231
313.15	0.4126	0.3781	0.8748	279.68	0.4232	0.8934400	4.106	4.211
318.15	0.4096	0.4135	0.8634	311.31	0.4224	0.9788172	4.076	4.204
323.15	0.4077	0.4491	0.8519	342.88	0.4231	1.0613600	4.054	4.208

[a]Standard uncertainties u are: $u(T)$=0.01K; $u(\beta_S)$=0.008%; $u(\alpha_P)$=(0.05-0.10)%; $u(\beta_T)$=(0.2-0.4)%; $u(C_V)$=(2-3) %; $u(C_P)$=(3-4)%.

Table 8: Enthalpy difference, $\Delta H = H(T) - H_0(T_0)$, of geothermal fluids (T_0 =273.15 K)

T (K)	ΔH (kJ·kg^{-1})	T (K)	ΔH (kJ·kg^{-1})	T (K)	ΔH (kJ·kg^{-1})	T (K)	ΔH (kJ·kg^{-1})
Izberbas (No. 68)		Izberbas (No. 129)		Thernair (No. 27T)		Thernair (No. 38T)	
278.15	21.251	278.13	21.430	278.14	21.364	278.14	21.671
283.15	42.361	283.15	42.927	283.15	42.697	283.15	43.322
293.15	84.257	293.15	85.493	293.14	84.928	293.15	86.231
303.15	125.87	303.15	127.82	303.15	126.96	303.15	128.82
313.15	167.40	313.15	170.03	313.15	168.83	313.15	171.20
323.15	209.02	318.15	191.13	323.10	210.47	318.15	192.33
333.15	250.91	323.15	212.25	333.15	252.711	323.15	213.44
-	-	333.15	254.60	-	-	-	-

[a]Standard uncertainties u are: $u(T)$=0.01K; $u(\Delta H)$=(2-4) %.

ACKNOWLEDGMENTS

I.M. Abdulagatov thanks the Applied Chemicals and Materials Division at the National Institute of Standards and Technology for the opportunity to work as a Guest Researcher at NIST during the course of this research. The authors thank Russian Scientific Fund (№14-19-00749) for the financial support.

REFERENCES

Abdulagatov, I.M., Dvoryanchikov, V.I., (1995). Thermodynamic properties of geothermal fluids. Russ. J. Geochem. 5, 612-620.

Abdulagatov, I.M., Abdulagatov, A.I., et al., (2005)a. Thermophyscal Properties of Pure Fluids and Aqueous Systems at High Temperatures and High Pressures, Begell House, Inc., New York.

Abdulagatov, I.M., Zeinalova, A.B., et al., (2005)b. Viscosity of aqueous Na2SO4 solutions at temperatures from 298 to 573 K and at pressures up to 40 MPa. Fluid Phase Equilibria, 227, 57-70.

Abdulagatov, I.M., Azizov, N.D. (2005)c. Densities, apparent molar volumes, and viscosities of concentrated aqueous $NaNO_3$ solutions at temperatures from 298 to 607 K and at pressures up to 30 MPa. J.Sol.Chem. 34, 645-685.

Abdulagatov, I.M., Azizov, N.D. (2006). Densities, apparent and partial molar volumes of concentrated aqueous LiCl solutions at high temperatures and high pressures. Chemical Geology 230, 22-41.

Abdulagatov, I.M., et al., (2007). Viscosities, densities, apparent and partial molar volumes of concentrated aqueous MgSO4 solutions at high temperatures and high pressures. Phys. Chem. Liq. 45, 127-148.

Abdulagatov, I.M., Assael, M., (2009). Viscosity. Hydrothermal Properties of Materials. Experimental Data on Aqueous Phase Equilibria and Solution Properties at Elevated Temperatures and Pressures, V.M. Valyashko, ed. John Wiley & Sons. London. Chapter 6, pp.249-270.

Abdulagatov, I.M., Akhmedova-Azizova, L.A., Aliev, R.M., Badavov, G.B. (2016). Measurements of the Density, Speed of Sound, Viscosity and Derived Thermodynamic Properties of Geothermal Fluids. J. Chem. Eng. Data, 61, 234–246.

Adams, J.J., Bachu, S., (2002). Equations of states for basin geofluids: algorithm review and intercomparison for brines. Geofluids 2, 257-271.

Alkan, H., Babadagli, T., et al., (1995). The prediction of the PVT/Phase behavior of the geothermal fluid mixtures. Proceeding of the World Geothermal Congress, IGA, pp. 1659-1665.

Ague, J.J., (2003). Fluid flow in the deep crust. Treatise of Geochemistry, The crust, editor RL Rudnick, Elsevier, Amstrdam, V.3, pp.195-228.

Aseyev, G.G., Zaytsev, I.D., (1996). Volumetric Properties of Electrolyte Solutions. Estimation Methods and Experimental Data. Begell-House, Inc., New-York.

Aseyev, G.G., (1998). Electrolytes. Properties of Solutions. Methods for Calculation of the Multicomponent Systems and Experimental Data on Thermal Conductivity and Surface Tension. Begell-House, Inc., New-York.

Battistelli, A., Calore, C., et al., (1993). A fluid property module for the TOUGH2 simulator for saline brines with non condensible gas. Proc.18th Workshop on Geothermal Reservoir Engineering, Stanford University, pp.249-259.

Battistelli, A., (2012). Improving the treatment of saline brines in EWASG for the simulation of hydrothermal systems. Proc. TOUGH Symp. 2012, Lawrence Berkeley Nat. Lab., Berkeley, California, pp.1-9.

Carvalho, P.J., Regueira, T., et al., (2010). Effect of Water on the Viscosities and Densities of 1-Butyl-3- methylimidazolium Dicyanamide and 1-Butyl-3-methylimidazolium Tricyanomethane at Atmospheric Pressure. J. Chem. Eng. Data 55, 645-652.

Champel, B., (2006). Discrepancies in brine density databases at geothermal conditions, Geothermics 35, 600-606.

DiGuilio, R.M., Teja, A.S., (1992). Thermal conductivity of aqueous salt solutions at high temperatures and high concentrations. Ind. Eng. Chem. Res. 31, 1081-1085.

DiGuilio, R.M., Lee, R.J., et al., (1990). Properties of lithium bromide-water solutions at high temperatures and concentrations-I. Thermal conductivity. ASHRAE Trans. 96, 702-708.

Dittman, G.L., (1977). Calculation of brine properties, Lawrence Livermore Laboratory, Report UCID 17406.

Dolejs, D., Manning, C.E., (2010). Thermodynamic model for mineral solubility in aqueous fluids: theory, calibration and application to model fluid-flow systems. Geofluids 10, 20-40.

Erday-Gruz, T., (1974). Transport Phenomena in Aqueous Solutions, John Wiley & Sons Inc., New York.

Ershaghi, I., Abdassah, D., et al., (1983). Estimation of geothermal brine viscosity. J. Pet. Tech. 35, 621-628.

Francke, H., Thorade, M., (2010). Density and viscosity of brine: An overview from a process engineers perspective. Chem. Erde, Geochem. 70, 23-32.

Francke, H., Kraume, M., et al., (2013). Thermal –hydraulic measurements and modelling of the brine circuit in a geothermal well. Envir. Earth Sci. 70, 3481-3495.

Golabiazar, R., Sadeghi, R. (2014). Salt-effects in aqueous surface-active ionic liquid 1-dodecyl-3-methylimidazolium bromide solutions: Volumetric and compressibility property changes and critical aggregation concentration shifts. J. Chem. Thermodyn. 76, 29-44.

Glasstone, S., Laidler, K., et al., (1941). Theory of Rate Processes, McGraw-Hill, New York.

Haas, J.L.Jr., (1976)a. Physical properties of the coexisting phases and thermochemical properties of the H2O component in boiling NaCl solutions: U.S. Geol. Survey Bull. 1421-A, 73 p.

Haas, J.L.Jr., (1976)b. Thermodynamic properties of the coexisting phases and thermochemical properties of the NaCl component in boiling NaCl solutions: U.S. Geol. Survey Bull. 1421-B, 71 p.

Helgeson, H.C., (1967). Solution chemistry and metamorphism. Res. Geochem., P.H. Abelson, ed. 55, 379-385.

Horvath, A.L., (1985). Handbook of Aqueous Electrolyte Solutions. Physical Properties, Estimation Methods and Correlation Methods. Ellis Horwood, West Sussex, England.

Huber, M.L., Perkins R.A., et al. (2009). New International formulation for the viscosity of H2O. J. Phys. Chem. Ref. Data 38, 101-125.

Huber, M.L., Perkins R.A., et al. (2012). New International formulation for the thermal conductivity of H2O. J. Phys. Chem. Ref. Data 41, 033102-1- 033102-23.

Kestin, J., Shankland, I.R., (1984). Viscosity of aqueous NaCl solutions in the temperature range 25-200 °C and in the pressure range 0.1-30 MPa. Int. J. Thermophys. 5, 241-263.

Kratky, O., Leopold, H., et al., (1969). Determination of density of liquids and gases to an accuracy of 10-6 g/cm3, with a sample volume of only 0.6 cm3. Zeitschrift für Angewandte Physik, **27**, 273-277.

Kratky, O., Leopold, H., et al., (1980). DMA45 Calculating Digital Density Meter, Instruction Manual. Digital Densimeter of Liquids and Gases (Paar A, KG, A-8054, Graz, Austria), pp.1-12.

Kroger, D., (2002/2003). Stabinger Viscometer. Petro Industry News, vol. 3, issue 4, Annual Buyers Guide.

Lee, K.S., (2000). Comparison of correlation equations for estimating brine properties under high pressure and temperature condition. Geosystem Eng. 3, 113-116.

Lemmon, E.W., Huber, M.L., et al., (2010). NIST Standard Reference Database 23, NIST Reference Fluid Thermodynamic and Transport Properties, REFPROP, version 9.0, Standard Reference Data Program,

National Institute of Standards and Technology: Gaithersburg, MD. Leopold, H., (1970). Electronik 297, 411-415.

McCain, Jr. W.D., (1991). Reservoir fluid property correlations-State of Art. Society of Petroleum Eng. Res. Eng., May, 266-272.

McKibbin, R., McNabb, A., (1995). Mathematical modeling the phase boundaries and fluid properties of the system H_2O+NaCl+CO_2. Proc. 17th New Zealand Geothermal Workshop, University of Auckland, pp.255-262.

Milsch, H., Kallenberg, B., et al., (2010). Mixing-rules of viscosity, electrical conductivity and density of NaCl, KCl, and CaCl2 aqueous solutions derived from experiments. EGU2010-1584, EGU General Assambly-2010, Geophys. Res. Abst., 12.

Muller, P.I.N., Weare, J.H., (1999), Model of Geothermal Brine Chemistry. Final Report, Grant DE-FG07-93ID13247, pp. 1-23.

Oldenburg, C., Pruess, K., et al., (1995). Heat and mass transfer in hypersaline geothermal systems. Proceeding of the World Geothermal Congress, IGA, pp. 1647-1652.

Ostermann, R.D., Paranjpe, S.G.,et al., (1986). The effect of dissolved gas on geothermal brine viscosity. Proc. 56th Ann. Soc. Petrol. Eng. California Regional Meeting, pp.381-389.

Palliser, Ch., McKibbin, R., (1998)a. A Model for deep Geothermal brines, III: Thermodynamic properties-enthalpy and viscosity. Transport in Porous Medias 33, 155-171.

Palliser, Ch., McKibbin, R., (1998)b. A Model for deep Geothermal brines, II: Thermodynamic properties-density, Transport in Porous Medias 33, 129-154.

Palliser, Ch., (1998). A model for deep geothermal brines: State space description and thermodynamic properties. Ph.D. Thesis, Massey University.

Piwinskii, A.J., Netherton, R., et al., (1977). Viscosity of brines from the Salton sea Geothermal Field, Imperial valley, California, Lawrence Livermore Laboratory, Report UCRL 52344, University of California, California.

Potter, R.W., Haas, J.L.Jr., (1977). A model for the calculation of the thermodynamic properties of geothermal fluids, Geothermal Resources Council, Transactions 1, 243-244.

Riedel, L., (1951). The heat conductivity of aqueous solutions of strong electrolytes. Chem. Ing. Tech. 23, 59-64.

Reindl, J., Shen, H., et al., (2009). Reservoir Engineering: An Introduction and Application to rico, Colorado, Geothermal Energy-MNGN598.

Rogers, P.S.Z., Pitzer, K.S., (1982), Volumetric properties of aqueous sodium chloride solutions. J. Phys. Chem. Ref. Data 11, 15-81.

Saadat, A., Frick, S., et al., (2008). Niedertemperaturstromerzeugung-systembetrachtung unter berücksichtigung des eigenbedarfs, in: Geothermische Technologien: Vom reservoir zur kilowattstunde; Tagung Potsdam, 27, und 28. Februar (2008) /VDI-Gesellschfat Energietechnik, VDI. Pp. 155-167.

Schmidt, H., Stephan,M., et al., (2012). Thermophysical properties of 1-ethyl-3-methylimidazolium ethyl sulfate. J. Chem. Thermodyn. 47, 68-75.

Schröder, E., Thomauske, K., et al., (2015). Design and test of a new calorimeter for online detection of geothermal water heat capacity. Geothermics 53, 202-212.

Segovia, J.J., Fandiño, O., et al., (2009). Automated densimetric system: Measurements and uncertainties for compressed systems. J. Chem. Thermodyn. 41, 632-638.

Spycher, N., Pruess, K., (2011). A model for thermophysical properties of CO_2-brine mixtures at elevated temperatures and pressures. In: Proc. 36th Workshop on Geothermal Reservoir Engineering, Stanford University, Stanford California, SGP-TR-191.

Stabinger, H., Kratky, O., et al. (1967). Eine neue ra isionsmethode ur estim-mun der ichte von lu ssi keiten. Monatshefte für Chemie. 98, 436-438.

Stabinger, H., (1994). Density Measurement Using Modern Oscillating Transducers, Yorkshire Trading Standards Unit, Sheffield.

Stefánsson, A., Driesner, Th., et al. (eds.), (2012). Thermodynamic of Geothermal Fluids, Mineralogical Society of America & Geochemical Society, Vol. 76.

Stokes, R.H., Mills, R., (1965). Viscosity of Electrolytes and Related Properties, Pergamon Press, New York.

Tariq, M., Carvalho, P.J., et al., (2011). Viscosity of (C2–C14) 1-alkyl-3-methylimidazolium bis(trifluoromethylsulfonyl) amide ionic liquids in an extended temperature range. Fluid Phase Equilib. 301, 22-32.

Vargaftik, N.B., Osminim, Y.P., (1956). Teploenergetika, 7, 11-15.

Wagner, W., Pruß, A., (2002). New international formulation for the thermodynamic properties of ordinary water substance for general and scientific use. J. Phys. Chem. Ref. Data 31, 387-535.

Wahl, E.F., (1977). Geothermal Energy Utilization. NY, Wiley.

Zezin, D., Driesner, Th., et al., (2014). Volumetric properties of mixed electrolyte aqueous solutions at elevated temperatures and pressures. The systems CaCl2-NaCl-H2O and MgCl-NaCl-H2O to 523.15, 70 Ma, and ionic stren th from (0.1 to 18) mol·k -1. J. Chem. Eng. Data (in press).